

Size control and its mechanism of SnAg nanoparticles

Wei-peng ZHANG^{1,2}, Chang-dong ZOU^{2,3}, Bing-ge ZHAO^{1,2}, Qi-jie ZHAI², Yu-lai GAO^{1,2}

1. Laboratory for Microstructures, Shanghai University, Shanghai 200436, China;
2. School of Materials Science and Engineering, Shanghai University, Shanghai 200072, China;
3. Institute of Research of Iron and Steel, Zhangjiagang 215625, China

Received 17 April 2013; accepted 7 May 2013

Abstract: Sn_{3.5}Ag (mass fraction, %) nanoparticles were synthesized by an improved chemical reduction method at room temperature. 1,10-phenanthroline and sodium borohydride were selected as the surfactant and reducing agent, respectively. It was found that no obvious oxidation of the synthesized nanoparticles was traced by X-ray diffraction. In addition, the results show that the density of primary particles decreases with decreasing the addition rate of the reducing agent. Moreover, the slight particle agglomeration and slow secondary particle growth can result in small-sized nanoparticles. Meanwhile, the effect of surfactant concentration on the particle size can effectively be controlled when the reducing agent is added into the precursor at an appropriate rate. In summary, the capping effect caused by the surfactant molecules coordinating with the nanoclusters will restrict the growth of the nanoparticles. The larger the mass ratio of the surfactant to the precursor is, the smaller the particle size is.

Key words: Sn_{3.5}Ag; size control; nanoparticles; chemical reduction method

1 Introduction

Nano-sized materials have attracted more and more attention in both science and technology fields recently. Because of their infinitesimal sizes, nanoparticles possess many unique properties which are different from those of their corresponding bulk materials, such as melting temperature depression. It has been sufficiently proved that the melting temperatures of metals can be lowered by decreasing their particle sizes down to nanometer range [1–6]. In electronic industry, the size dependence of melting temperature has drawn adequate attention to lower the melting point of environmentally friendly lead-free solders, such as Sn–Ag based alloy, which is one of the promising alternatives to replace the traditional Sn–Pb solder [7–9].

To better understand the size effect, various methods have been developed to fabricate metal nanoparticles. BENJAMIN [10] has manufactured Ni-based alloy nanoparticles by mechanical alloying in the last 1960s for the first time. Then physical vapor deposition was used to prepare nanoparticles of Pd, Cu, and Fe by BIRINGER et al [11]. The recently

developed technology was direct current arc method, which was successfully applied in various metals and alloys [12,13]. In particular, chemical reduction method of the oxidation–reduction reaction among ions in the solution was widely used in experimental studies [2–4,14,15].

Sn–Ag based nanoparticles, which were concerned in our study, were successfully fabricated through chemical reduction method by some researchers. JIANG et al [7] fabricated Sn_{3.5}Ag nanoparticles by low-temperature chemical reduction method and analyzed their size-dependent melting temperature. However, in their study, the reactions took place at the temperature of –20 °C and were protected by inert gases, which would limit the practical applications of this technique. HSIAO and DUH [16] also used chemical reduction method to synthesize Sn–3.5Ag–xCu (x=0.2, 0.5, 1.0) nanoparticles, and NaBH₄ was applied as the reducing agent. In our previous work, Sn_{3.5}Ag nanoparticles were prepared via chemical reduction method at room temperature in the atmospheric environment, yet only nanoparticles with a large size distribution were obtained [17]. To conduct a systematic research into size effect, nanoparticles with a broader size range and a smaller size distribution are

especially studied. However, little work has been performed to control the size of Sn_{3.5}Ag nanoparticles during the chemical synthesis process.

In this work, an improved chemical reduction method was developed. The size control of Sn_{3.5}Ag nanoparticles and the theoretical analysis under different synthesis conditions were focused. Though the melting temperature depression of as-synthesized Sn_{3.5}Ag nanoparticles was not involved, the size control strategies in the present work did make sense in both theoretical study and practical application.

2 Experimental

Sodium borohydride (NaBH₄), 1,10-phenanthroline (C₁₂H₈N₂·H₂O), anhydrous ethanol (CH₃CH₂OH) were used as reducing agent, surfactant, solvent, respectively. The tin(II) 2-ethylhexanoate (C₁₆H₃₀O₄Sn) and silver nitrate (AgNO₃) were mixed as a precursor.

In a typical synthesis process, 0.2998 g tin (II) 2-ethylhexanoate, 0.0051 g silver nitrate and 0.1110 g 1,10-phenanthroline were mixed into 60 mL anhydrous ethanol solution to synthesize SnAg1, as listed in Table 1. The mixture was electromagnetic alloy stirred for 2 h in the atmospheric environment. Then 0.1892 g sodium borohydride was added into the solution and mechanically stirred for another 1 h until the termination of the reaction. The obtained nanoparticles were precipitated by a centrifuge at 4000 r/min for 20 min and then rinsed 3 times with anhydrous ethanol. Finally, the nanoparticles were placed in vacuum drying chamber and dried at 40 °C for 8 h.

The crystal structure of the Sn–Ag nanoparticles was examined by X-ray diffraction (XRD) using Cu K_α radiation ($\lambda=0.154056$ nm) on a Rigaku D/Max–2550 X-ray diffractometer.

Field emission scanning electronic microscope (FE-SEM, model JSM–6700F) was used to investigate the morphology of the synthesized nanoparticles. The SEM specimens were prepared by placing a few drops of the solution containing nanoparticles onto the silicon substrate. High resolution transmission electron microscope (HRTEM, model JSM–2010F) was employed to analyze the microstructure of the as-synthesized Sn–Ag nanoparticles.

3 Results and discussion

3.1 Influence of surfactant concentration on directly added reducing agent

The synthesis parameters with different concentrations of surfactant are listed in Table 1 and the reducing agent is directly added into the solution.

Table 1 Synthesis parameters for preparing nanoparticles

Sample	Mass/g			Volume/mL	
	C ₁₆ H ₃₀ O ₄ Sn	AgNO ₃	C ₁₂ H ₈ N ₂ ·H ₂ O	NaBH ₄	CH ₃ CH ₂ OH
SnAg1	0.2998	0.0051	0.1110	0.1892	60
SnAg2	0.2998	0.0051	0.1586	0.1892	60
SnAg3	0.2998	0.0051	0.2180	0.1892	60
SnAg4	0.2998	0.0051	0.2775	0.1892	60

The XRD patterns of as-prepared SnAg alloys nanoparticles are shown in Fig. 1. Tetragonal β -Sn (JCPDS No. 65–2631) and orthorhombic Ag₃Sn (JCPDS No. 71–0530) can be matched in all the four samples. Diffraction peaks of Ag₃Sn in the patterns indicate the successful alloying of Ag and Sn. In particular, no visible oxidation peak is observed in the XRD patterns, implying that the chosen surfactant can effectively prevent the nanoparticles from oxidation even in the atmospheric environment.

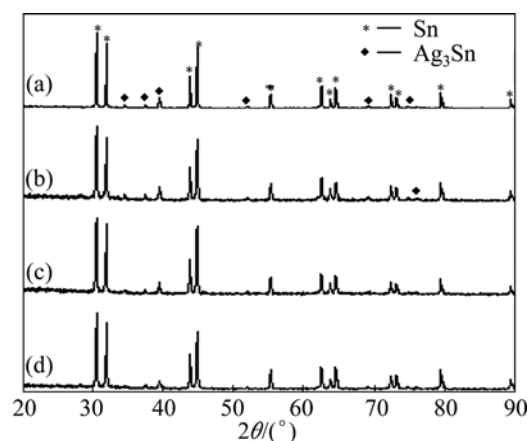


Fig. 1 XRD patterns of as-prepared SnAg nanoparticles: (a) SnAg1; (b) SnAg2; (c) SnAg3; (d) SnAg4

The morphology of the four samples was observed by FE-SEM. Figure 2 shows the secondary electron images of the synthesized SnAg nanoparticles. With the lowest surfactant concentration, SnAg1 reveals largest particle size and most irregular shapes in all samples. As the surfactant increases, there is no significant difference in morphology and particle size among SnAg2, SnAg3 and SnAg4.

Solid NaBH₄ powders used as reducing agent were generally directly added into the precursor solution. In this condition a lot of gas was produced and temperature of the solution was increased. After 2 min, no gas released further and the temperature of solution returned to normal. This phenomenon demonstrates that the reactants reacted violently at the first 2 min as soon as the reducing agent was added.

In the initial stages of the reaction, a plenty of clusters were formed in the system. The reaction was so violent that there was no time for the capping effect of surfactant to act [18,19] on the clusters. Thus, clusters were likely to aggregate and grow up to larger nanoparticles. As a result, it could be inferred from the FE-SEM images that the morphology and size of Sn_{3.5}Ag nanoparticles could not be effectively controlled by increasing the surfactant concentration alone when the reducing agent was added straightway.

3.2 Influence of addition rate of reducing agent

Based on the above-mentioned analysis, the reaction was too drastic to control the morphology and particle size in the case of adding reducing agent directly. To optimize this process, the addition rate of reducing agent was changed. NaBH₄ was firstly mixed with anhydrous alcohol to get a homogeneous solution. Then the reducing agent was added into the precursor solution by means of dropping. Different dropping times, as listed in

Table 2, were designed to investigate the influence of additive rate of reducing agent on the nanoparticles. The dropping times of SnAg5, SnAg6, SnAg7 and SnAg8 were 0, 11, 20 and 38 min, respectively.

Figure 3 shows the FE-SEM images of the synthesized Sn_{3.5}Ag nanoparticles with different dropping times. Nanoparticles with nearly spherical shape were formed, together with a few cube shaped ones.

The size distribution of nanoparticles was analyzed by FE-SEM. For the four samples mentioned above, the statistical distribution of particle sizes is shown in Fig. 4. It is found that the percentage of nanoparticles less than 50 nm increases with longer dropping time. Similarly, the same trend could be found from particles less than 100 nm. However, the proportion of particles larger than 100 nm decreases rapidly with increasing dropping time. In addition, the average diameter of the manufactured nanoparticles decreases drastically with increasing dropping time.

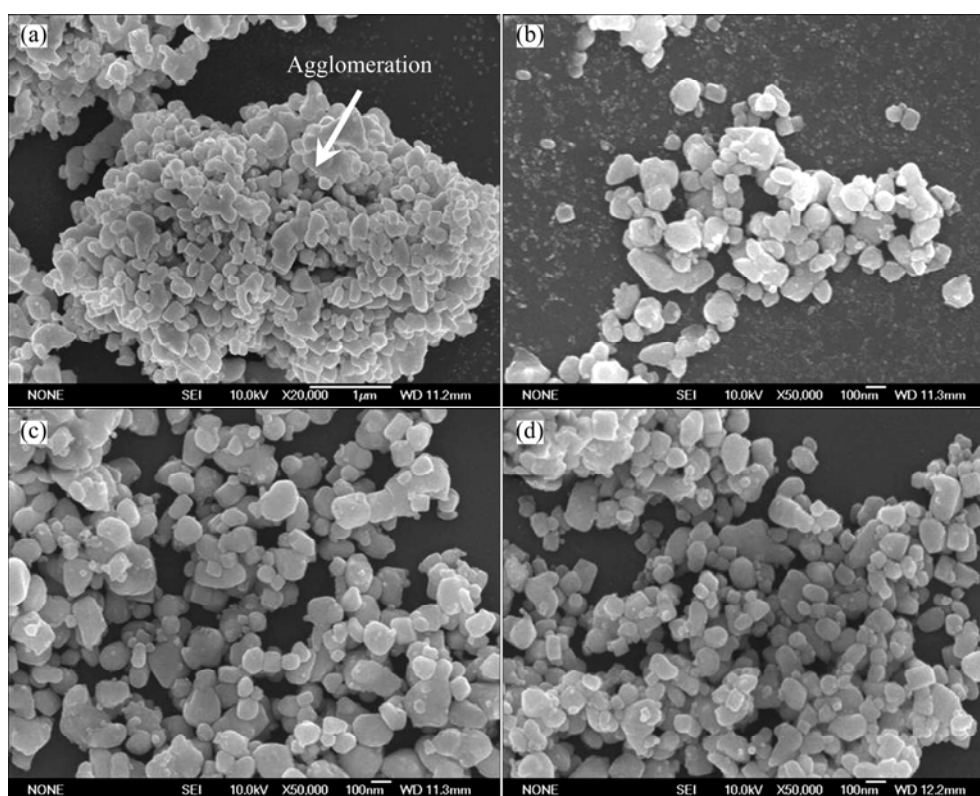


Fig. 2 FE-SEM images of as-prepared Sn_{3.5}Ag nanoparticles: (a) SnAg1; (b) SnAg2; (c) SnAg3; (d) SnAg4

Table 2 Synthesis parameters in case of different dropping time of NaBH₄

Sample	Mass/g			Volume/mL		Dropping time/min
	C ₁₆ H ₃₀ O ₄ Sn	AgNO ₃	C ₁₂ H ₈ N ₂ ·H ₂ O	NaBH ₄	CH ₃ CH ₂ OH	
SnAg5	0.2998	0.0051	0.2775	0.1892	50	0
SnAg6	0.2998	0.0051	0.2775	0.1892	50	11
SnAg7	0.2998	0.0051	0.2775	0.1892	50	20
SnAg8	0.2998	0.0051	0.2775	0.1892	50	38

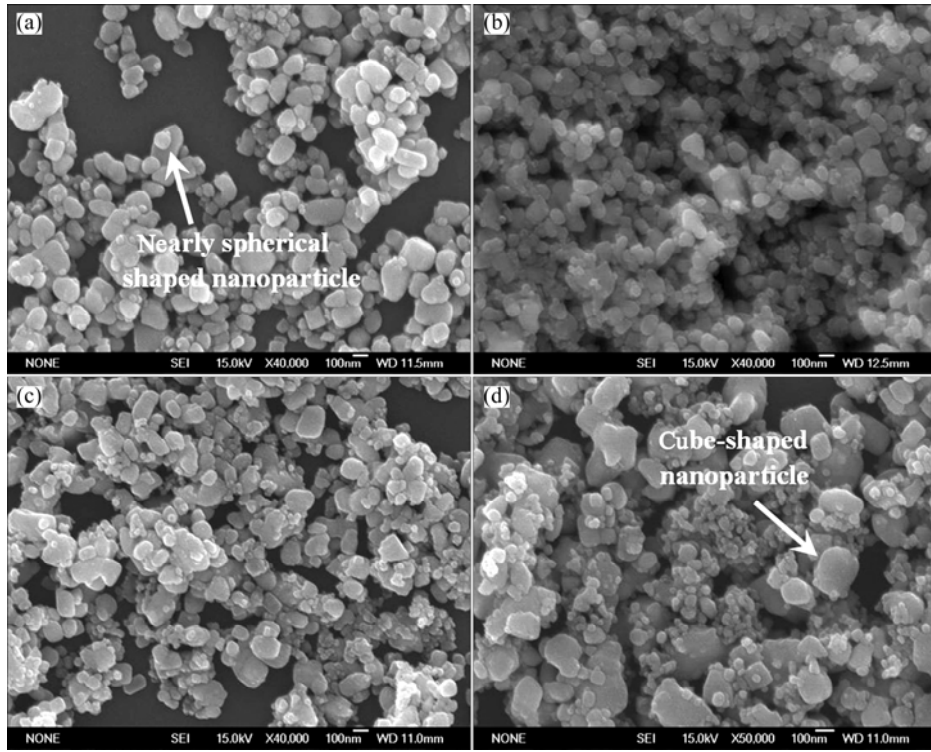


Fig. 3 FE-SEM images of Sn_{3.5}Ag nanoparticles with different dropping times of reducing agent: (a) SnAg₅; (b) SnAg₆; (c) SnAg₇; (d) SnAg₈

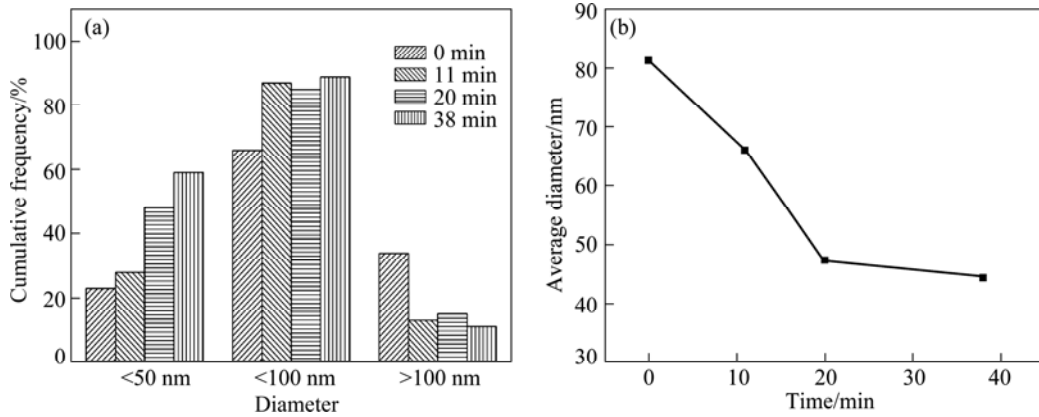


Fig. 4 Percent of nanoparticles in different sizes (a) and relationship between average diameter and dropping time (b)

The formation rate of the primary particles and the secondary particles in the solution could be calculated via the method suggested by PRIVMAN et al [20]. The formation rate of secondary particles was expressed by

$$\frac{dN_s(t)}{dt} = w_{s-1}N_{s-1}(t) - w_s(t)N_s(t), \quad s > 1 \quad (1)$$

where t is the time; $N_s(t)$ is the time-dependent number density (per unit volume) of the secondary particle consisting of s primary particles; and $w_s(t)$ is the attachment rate [21] as follows:

$$w_s(t) = 4\pi R_s D N_1(t) \quad (2)$$

where D is the diffusion constant; and R_s is the radius of the secondary particles, given by

$$R_s = 1.2rs^{1/3} \quad (3)$$

where r is the primary particle radius which depends on the experimental data; $N_1(t)$ is the number density (per unit volume) of the primary particles. The expression of $N_1(t)$ could be written as

$$N_1(t) = \int_0^t \rho(t') dt' - \sum_{j=2}^{\infty} j N_j(t) \quad (4)$$

where t' is the time; $\rho(t')$ is the generation rate of the primary particles.

From Eqs. (2) and (4), it is clear that the formation rate of the primary particles $\rho(t')$ would affect their attachment rate $w_s(t)$. And the attachment rate $w_s(t)$ could influence the formation rate of the secondary particles $dN_s(t)/dt$, which could be concluded from Eq. (1).

Therefore, the formation rate of both kinds of particles would affect the size distribution of the final synthesized nanoparticles. To get a better control on nanoparticle size, the nucleation process of primary particles should be faster and the growth process of secondary particles should be slower.

In fact, the formation rate of these two kinds of particles is influenced by the reactant concentrations. ZHANG et al [14] found that the amount of copper nuclei rose with the increased initial concentration of Cu^{2+} , and smaller size particles were obtained then. However, agglomeration of the nuclei would appear when the reactant concentration was too high, which resulted in large secondary particles. Similar results were obtained by WANG et al [22] in the size control of Co nanoplatelets. Besides, the results also show that high dosages of reducing agent would increase the reaction kinetics and thus more nuclei of Co crystals and smaller Co nanoplatelets could be formed.

In the present study, however, the reaction was so intense when the dropping time of reducing agent was 0

min. High concentration of reactants produced too many primary particles which were tendency to aggregate with each other and form large secondary particles. With decreasing addition rate of reducing agent, the reactant concentration became smaller. The agglomeration process was moderate then. So the smaller secondary particles could be obtained, as shown in Fig. 4. Thus, the size and size distributions of Sn_{3.5}Ag particles were correspondingly controlled in this way.

3.3 Influence of surfactant concentration with gradually added reducing agent

The influence of surfactant concentration on the size control of SnAg nanoparticles was discussed when the reducing agent was dropped into the solution gradually. The dropping time was the same as sample SnAg7, i.e. 20 min.

Table 3 lists the synthesis parameters of samples used for FE-SEM analysis. Figure 5 shows the FE-SEM images of the synthesized nanoparticles with different amounts of surfactant. It can be seen that the size of

Table 3 Synthesis parameters of samples with different surfactant contents

Sample	Mass/g				Volume/mL
	$\text{C}_{16}\text{H}_{30}\text{O}_4\text{Sn}$	AgNO_3	$\text{C}_{12}\text{H}_8\text{N}_2\cdot\text{H}_2\text{O}$	NaBH_4	$\text{CH}_3\text{CH}_2\text{OH}$
SnAg9	0.2998	0.0051	0.2775	0.1892	50
SnAg10	0.2998	0.0051	0.5550	0.1892	50
SnAg11	0.2998	0.0051	0.8325	0.1892	50
SnAg12	0.2998	0.0051	1.1100	0.1892	50

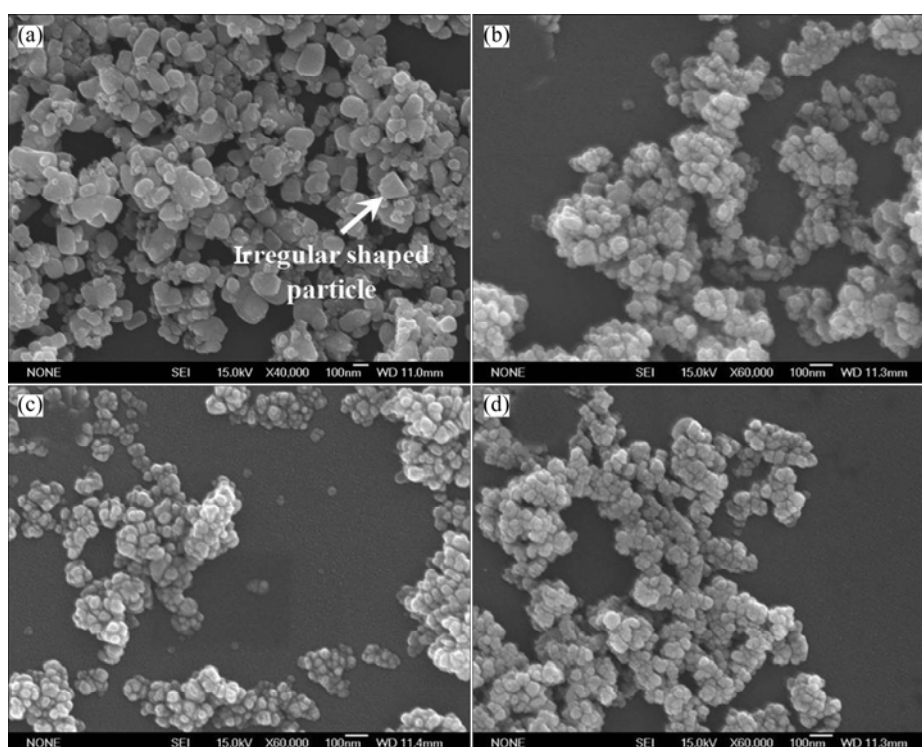


Fig. 5 FE-SEM images of synthesized Sn_{3.5}Ag nanoparticles with different surfactant concentrations: (a) SnAg9; (b) SnAg10; (c) SnAg11; (d) SnAg12

Sn_{3.5}Ag nanoparticles decreases significantly with increasing surfactant content. There are a few irregular shaped particles in addition to spherical particles in SnAg₉, corresponding to the lowest surfactant content 0.2775 g. As for SnAg₁₀, SnAg₁₁ and SnAg₁₂, the morphologies of nanoparticles are mostly spherical and no irregular particles appear.

The relationship between the surfactant content and the average diameter of nanoparticles, as well as the percent of particles with different sizes in the samples, are shown in Fig. 6. Along with the increase of surfactant content, the average diameter of nanoparticles is significantly reduced and smaller size distribution is obtained.

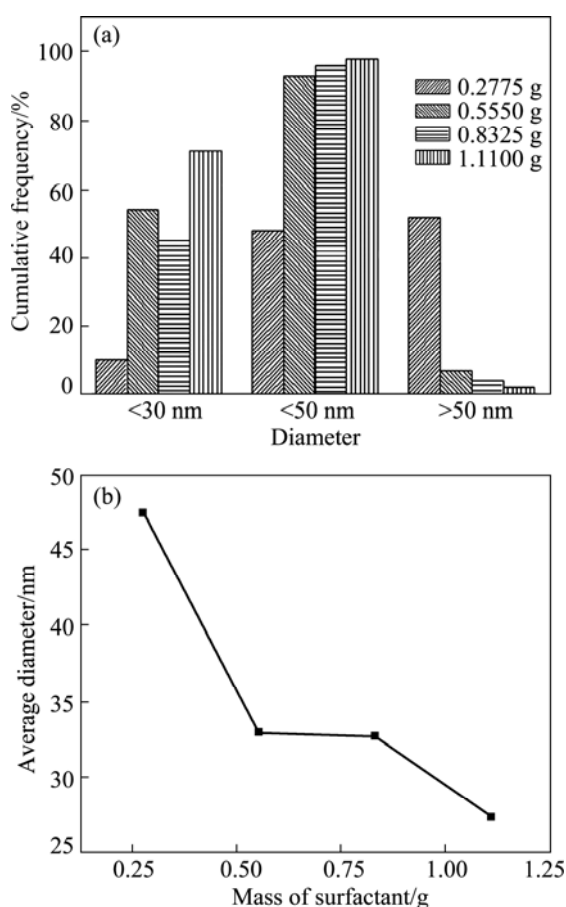


Fig. 6 Percentage of nanoparticles in different sizes (a) and relationship between average diameter and surfactant contents (b)

It is well known that surfactant plays an important role in the chemical synthesis method. WANG et al [23,24] studied the synthesis process of SnO₂ nanorods. In their study, 1,10-phenanthroline and SnCl₄, used as surfactant and precursor respectively, were well-stirred in the aqueous solution, in which coordination compound (phen)SnCl₄ (phen stands for 1,10-phenanthroline) was formed. The reducing agent NaBH₄ was added into the system afterwards and reacted with (phen)SnCl₄. The Sn

nanoparticles were encapsulated by 1,10-phenanthroline. The similar results were obtained for Ag nanoparticles [25–27]. Other researchers reported that 1,10-phenanthroline, acted as complexing agent, coordinated with metal through nitrogen-atoms [18,19]. In our previous work, 1,10-phenanthroline was applied to controlling the size, morphology, and oxidation of Sn_{3.0}Ag_{0.5}Cu nanoparticles [28], which was an extensively used method in chemical synthesis process [29,30]. The higher the concentration of the surfactant was, the smaller the particle size was [31–33].

Therefore, the role of the surfactant used in this section could be summarized as follows. In the pre-mixing process, 1,10-phenanthroline coordinated with the ions in the precursor solution. And the metal ions in the complex compounds were reduced when NaBH₄ was added. Then the coordination between the surface atoms of the nanoparticles and 1,10-phenanthroline occurred, as shown in Fig. 7. It was the passivation layer of surfactant that prohibited the Sn_{3.5}Ag nanoparticles from growing and aggregating. The higher the content of 1,10-phenanthroline was, the stronger the effect of this coordination was. Thus, the size of Sn_{3.5}Ag nanoparticles could be controlled by the surfactant addition and improved synthesis process.

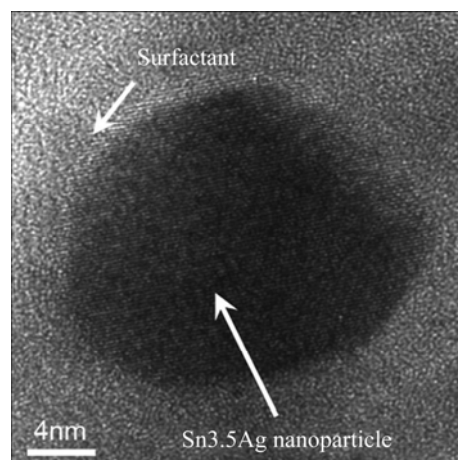


Fig. 7 Typical HRTEM image of as-synthesized Sn_{3.5}Ag nanoparticles

4 Conclusions

1) Due to the intense reaction, the size of Sn_{3.5}Ag nanoparticles was hardly controlled by only changing the surfactant concentration if the reducing agent was added into the precursor solution directly.

2) Too many primary particles would be produced with rapid reducing agent addition rate. And the agglomeration and secondary particle growth were serious then. At last, large nanoparticles were obtained. The results reveal that the required Sn_{3.5}Ag nanoparticles could be obtained when the dropping time

of NaBH_4 was optimized.

3) The selected surfactant could successfully govern the particle size when the reducing agent was added by dropping. With increasing the surfactant content, the average size of the as-synthesized nanoparticles was significantly reduced and the size distribution was also narrowed.

References

- [1] YASUDA H, MITSUISHI K, MORI H. Particle-size dependence of phase stability and amorphouslike phase formation in nanometer-sized Au–Sn alloy particles [J]. *Physical Review B*, 2001, 64: 094101.
- [2] ZOU Chang-dong, GAO Yu-lai, YANG Bin, ZHAI Qi-jie. Size-dependent melting properties of Sn nanoparticles by chemical reduction synthesis [J]. *Transactions of Nonferrous Metals Society of China*, 2010, 20: 248–253.
- [3] WEI Su-feng, JIANG Qing, LIAN Jian-she. Synthesis and characteristics of large-scale ZnO rods by wet chemical method [J]. *Transactions of Nonferrous Metals Society of China*, 2008, 18: 1089–1093.
- [4] BHAGATHSINGH W, NESARAJ A S. Low temperature synthesis and thermal properties of Ag–Cu alloy nanoparticles [J]. *Transactions of Nonferrous Metals Society of China*, 2013, 23: 128–133.
- [5] LITTLE SA, BEGOU T, COLLINS RW, MARSILLAC S. Optical detection of melting point depression for silver nanoparticles via in situ real time spectroscopic ellipsometry [J]. *Applied Physics Letters*, 2012, 100: 051107.
- [6] LUO Wen-hua, SU Ka-lin, LI Ke-min, LIAO Gao-hua, HU Neng-wen, JIA Ming. Substrate effect on the melting temperature of gold nanoparticles [J]. *The Journal of Chemical Physics*, 2012, 136: 23470.
- [7] JIANG H, MOON K, HUA F, WONG C P. Synthesis and thermal and wetting properties of tin/silver alloy nanoparticles for low melting point lead-free solders [J]. *Chemistry of Materials*, 2007, 19: 4482–4485.
- [8] CHEN Hong-tao, HAN Jing, LI Jue, LI Ming-yu. Inhomogeneous deformation and microstructure evolution of Sn–Ag-based solder interconnects during thermal cycling and shear testing [J]. *Microelectronics Reliability*, 2012, 52: 1112–1120.
- [9] KIM I, KANG M, KIM SW, JUNG E, LEE S H. Thermal diffusivity of Sn–Ag–Cu-based, Pb-free, micro- and nano-sized solder balls [J]. *Thermochimica Acta*, 2012, 542: 42–45.
- [10] BENJAMIN J. Dispersion strengthened superalloys by mechanical alloying [J]. *Metallurgical and Materials Transactions B*, 1970, 1: 2943–2951.
- [11] BIRINGER R, GLEITER H, KLEIN H P, MARQUARDT P. Nanocrystalline materials an approach to a novel solid structure with gas-like disorder? [J]. *Physics Letters A*, 1984, 102: 365–369.
- [12] CHANG I H T, REN Z. Simple processing method and characterisation of nanosized metal powders [J]. *Materials Science and Engineering A*, 2004, 375–377: 66–71.
- [13] GAO Y, ZOU C, YANG B, ZHAI Q, LIU J, ZHURAVLEV E, SCHICK C. Nanoparticles of SnAgCu lead-free solder alloy with an equivalent melting temperature of SnPb solder alloy [J]. *Journal of Alloys and Compounds*, 2009, 484: 777–781.
- [14] ZHANG Qiu-li, YANG Zhi-mao, DING Bing-jun, LAN Xin-zhe, GUO Ying-juan. Preparation of copper nanoparticles by chemical reduction method using potassium borohydride [J]. *Transactions of Nonferrous Metals Society of China*, 2010, 20(s): s240–s244.
- [15] FU Yue-jiao, ZHANG Lu-yan, CHEN Gang. Preparation of a carbon nanotube-copper nanoparticle hybrid by chemical reduction for use in the electrochemical sensing of carbohydrates [J]. *Carbon*, 2012, 50: 2563–2570.
- [16] HSIAO Li-yin, DUH Jenq-gong. Synthesis and characterization of lead-free solders with Sn–3.5Ag–xCu ($x=0.2, 0.5, 1.0$) alloy nanoparticles by the chemical reduction method [J]. *Journal of the Electrochemical Society*, 2005, 152: J105–J109.
- [17] ZOU Chang-dong, GAO Yu-lai, YANG Bin, ZHAI Qi-jie. Synthesis and DSC study on Sn3.5Ag alloy nanoparticles used for lower melting temperature solder [J]. *Journal of Materials Science: Materials in Electronics*, 2010, 21: 868–874.
- [18] BRANDT W W, DWYER F P, GYARFAS E D. Chelate complexes of 1,10-phenanthroline and related compounds [J]. *Chemical Reviews*, 1954, 54: 959–1017.
- [19] GALLAGHER J, CHEN C H B, PAN C Q, PERRIN D M, CHO Y M, SIGMAN D S. Optimizing the targeted chemical nuclease activity of 1,10-phenanthroline–copper by ligand modification [J]. *Bioconjugate Chemistry*, 1996, 7: 413–420.
- [20] PRIVMAN V, GOIA D V, PARK J, MATIJEVIC E. Mechanism of formation of monodispersed colloids by aggregation of nanosize precursors [J]. *Journal of Colloid and Interface Science*, 1999, 213: 36–45.
- [21] WEISS G H. Overview of theoretical models for reaction rates [J]. *Journal of Statistical Physics*, 1986, 42: 3–36.
- [22] WANG Hua-zhi, ZHANG Lei, HUANG Juan-juan, LI Jian-gong. Facile synthesis and characterization of Co nanoplatelets with tunable dimensions via solution reduction process [J]. *Journal of Nanoparticle Research*, 2010, 13: 1709–1715.
- [23] WANG Y, LEE J Y, DEIVARAJ T C. Controlled synthesis of v-shaped SnO_2 nanorods [J]. *Journal of Physical Chemistry B*, 2004, 108: 13589–13593.
- [24] WANG Y, LEE J Y. Molten salt synthesis of tin oxide nanorods: morphological and electrochemical features [J]. *Journal of Physical Chemistry B*, 2004, 108: 17832–17837.
- [25] SARKAR S, PRADHAN M, SINHA A K, BASU M, PAL T. Chelate effect in surface enhanced raman scattering with transition metal nanoparticles [J]. *The Journal of Physical Chemistry Letters*, 2009, 1: 439–444.
- [26] MUNIZ-MIRANDA M. Surface enhanced raman scattering and normal coordinate analysis of 1,10-phenanthroline adsorbed on silver sols [J]. *The Journal of Physical Chemistry A*, 2000, 104: 7803–7810.
- [27] JANG N H, SUH J S, MOSKOVITS M. Effect of surface geometry on the photochemical reaction of 1,10-phenanthroline adsorbed on silver colloid surfaces [J]. *The Journal of Physical Chemistry B*, 1997, 101: 8279–8285.
- [28] ZOU Chang-dong, GAO Yu-lai, YANG Bin, ZHAI Qi-jie. Nanoparticles of Sn3.0Ag0.5Cu alloy synthesized at room temperature with large melting temperature depression [J]. *Journal of Materials Science: Materials in Electronics*, 2012, 23: 2–7.
- [29] SUBRAMANIAM C, TOM R T, PRADEEP T. On the formation of protected gold nanoparticles from AuCl_4^- by the reduction using aromatic amines [J]. *Journal of Nanoparticle Research*, 2005, 7: 209–217.
- [30] YANG You-ping, HUANG Ke-long, LIU Ren-sheng, WANG Li-ping, ZENG Wen-wen, ZHANG Ping-min. Shape-controlled synthesis of nanocubic Co_3O_4 by hydrothermal oxidation method [J]. *Transactions of Nonferrous Metals Society of China*, 2007, 17: 1082–1086.
- [31] PUNTES V F, KRISHNAN K M, ALIVISATOS A P. Colloidal nanocrystal shape and size control: The case of cobalt [J]. *Science*, 2001, 291: 2115–2117.
- [32] SCHMID G, CHI L F. Metal clusters and colloids [J]. *Advanced Materials*, 1998, 10: 515–526.
- [33] WANG Z L. Structural analysis of self-assembling nanocrystal superlattices [J]. *Advanced Materials*, 1998, 10: 13–30.

SnAg 纳米粒子的尺寸控制及其机制

张卫鹏^{1,2}, 邹长东^{2,3}, 赵炳戈^{1,2}, 翟启杰², 高玉来^{1,2}

1. 上海大学 微结构实验室, 上海 200436;
2. 上海大学 材料科学与工程学院, 上海 200072;
3. 江苏省(沙钢)钢铁研究院, 张家港 215625

摘要: 采用一种改进的化学还原法, 在室温下合成 Sn_{3.5}Ag (质量分数, %)纳米颗粒。实验所用表面活性剂和还原剂分别为邻啡罗琳和硼氢化钠。X 射线衍射分析表明所合成的纳米粒子没有明显的氧化现象。结果表明: 在反应物浓度较小时, 产生的一次粒子较少, 团聚及二次粒子生长程度较小, 纳米颗粒的尺寸也随之减小。当以某一合适的速率添加还原剂到前驱体溶液中时, 表面活性剂浓度对纳米颗粒尺寸起到控制作用。由于表面活性剂分子可以与纳米团簇之间产生配位作用, 因此可以抑制纳米颗粒的长大。表面活性剂与前驱体溶液质量的比值越大, 得到的纳米颗粒尺寸越小。

关键词: Sn_{3.5}Ag; 尺寸控制; 纳米颗粒; 化学还原法

(Edited by Chao WANG)